J. Phys. II France **4** (1994) 1557-1569 SEPTEMBER **1994,** PAGE 1557

Classification
Physics Abstracts
61.30 — 82.70 — 61.30J

On the dispersion of latex particles in a nematic solution. I. Experimental evidence and a simple model

P. Poulin, V. A. Raghunathan, P. Richetti and D. Roux

Centre de Recherche Paul Pascal, Avenue Schweitzer, 33600 Pessac, France

(*Received 9 February 1994, accepted in final form 24 May 1994*)

Résumé. — Des billes de latex sont suspendues dans une solution micellaire isotrope qui à basse température présente une phase nématique. Nous observons qu à la transition les billes sont admises dans la phase ordonnée ou en sont rejetées selon leur taille. Nous rendons compte de cette observation par un modèle à deux paramètres d'ordre couplés. Les diagrammes de phases expérimentaux et théoriques sont alors comparés dans le voisinage de la transition.

Abstract. — Latex polyballs are suspended in an isotropic micellar solution which exhibits a nematic phase at low temperatures. At the transition, we observe that the particles are either retained or expelled from the structured phase depending on their size. A mean field theory with two coupled order parameters is proposed to account for this behavior at the transition. The experimental and theoretical phase diagrams are in qualitative agreement.

1. Introduction.

Much attention has been focused on the stability of dispersions of colloidal particles in a fluid. Very early [1-5], reversible phase separations have been observed in these systems. Phase transitions in colloidal suspensions are divided into two classes ; i) disorder-order transitions occur in systems dominated by repulsive interparticle potentials [3-5] and ii) fluid-fluid or fluid-solid transitions leading to two coexisting phases take place when the interparticle potential is attractive [2, 6-9]. In regular systems the solvent is macroscopically isotropic and then the interactions mediated by it keep the same symmetry. An interesting intermediate situation arises when anisotropic interactions are induced by an applied field, for instance in hydrodynamic flows or electromagnetic fields. The interparticle potential may then be attractive along particular directions and repulsive along others, thus providing very original phases. For instance, in an applied electric or magnetic field, colloidal suspensions may become a homogeneous one phase suspension of flexible strings made up of linearly aggregated particles, like pearl chains [10-12].

An alternative procedure to generate such anisotropic interactions would be to suspend colloidal particles in an anisotropic medium, such as a liquid crystal. In addition to the

common interactions observed in isotropic solvents, at least three extra specific forces are expected in a structured fluid. The most intuitive of them is elastic in origin : every change in separation between two particles would modify the strain field in the structure and for weak distortions the liquid crystal would respond elastically by giving rise to an interaction between the particles [13, 14]. For instance in a nematic phase, the sign and the magnitude of the elastic interaction would depend both on the anchoring conditions on the colloidal surfaces and on the relative orientation of the displacement with respect to the local director of the mesophase. While the first interaction is related to the orientational distortion of the order parameter, the second one arises from the modification of its amplitude. Owing to specific wetting conditions of the solvent on the particles, a non-uniform distribution of the magnitude of the order parameter develops near each particle surface, over a distance of a few order parameter correlation lengths. The overlapping of the surrounding layers of two particles would cause an interaction between them [15-17]. The third interaction is even more subtle. This interaction arises from orientational fluctuations in anisotropic mesophases. Between two particles, the rigid boundary conditions suppress locally a number of fluctuating modes, namely those having a lateral extension larger than the separation between the particles [18]. The associated free energy decreases with decreasing separation between the surfaces. A remarkable feature is that this interaction can fall off more slowly than the van der Waals interaction and should become dominant at large separations.

On the other hand, the doping of a liquid crystal with dispersed colloidal particles has a great interest from both a fundamental and practical standpoint. From the former it is the means to impose a controlled density of defects in the long range organization. By coupling effects, one may suspect that the physical properties of the mesophase would be altered, notably its elastic moduli. Moreover the proliferation of defects is well-known to lead to phase transition [19] and theory predicts that the first order nematic-isotropic transition may then split into a pair of continuous transitions with a novel intermediate phase [20]. From a more practical viewpoint, attention has been paid recently to a new kind of liquid crystal displays based on nematic phases doped with small particles [21].

To our knowledge two kinds of experimental studies have been performed on nematic mesophases in which inclusions have been added.

The first ones have followed the Brochard-de Gennes predictions [22] to circumvent the limitation of high magnetic field required to orient liquid crystals exhibiting a very weak anisotropy of diamagnetic susceptibility. They proposed doping the liquid crystal matrix with well-dispersed anisotropic ferromagnetic grains. At some critical ferrofluid concentration, the liquid crystalline matrix is oriented by the magnetic grains resulting in a mechanical coupling. The strength of the magnetic field required to orient the whole sample is then reduced by many orders of magnitude. In spite of many attempts only a few have succeeded in realization of these systems [23, 24]. The difficulty is to maintain the particles dispersed in order to get the collective behavior. Usually, the particles cluster even in the highly dilute regime.

Very recently a second type of systems has been investigated in order to obtain bistable liquid crystal displays already mentioned above [21]. The material consists of small solid inorganic particles (silica spheres) dispersed in thermotropic nematic phases. Inside the dispersion, the particles form agglomerates without leading to phase separation. In terms of light scattering, they are bistable with a first transparent state under homeotropic alignment and a second scattering state without alignment (randomly aligned). The doping particles facilitate a fast local switching from one state to the other either by a two-frequency addressing technique or by thermal exchange from a focused laser beam. The reasons as to why the aggregates allow the matrix to remain in a transparent homeotropic state on removal of the aligning electric field are not yet well understood. Once the writing is performed thermally by

switching back to the strongly scattering state with a focused laser beam, a fast erasure is obtained by applying the electric field again.

In the present paper, we study the stability of a suspension of small particles dispersed in a nematic medium. First, in an experimental section, we describe the phase diagrams obtained with a lyotropic system and spherical lattices of 1 200 Å and 600 Å diameter. With the larger particles, a phase separation process occurs at the isotropic-nematic transition, expelling every particle from the nematic phase into the isotropic phase. On the other hand, the smaller particles are kept dispersed in the nematic phase up to a few percent in concentration. They remain Brownian even in the nematic phase. A comparison of dynamic light scattering results obtained in the isotropic and nematic phases show that the particles are well-dispersed over an extended domain in the nematic phase. To describe the stability near the isotropic transition, we develop in section 3 a very simple model (Landau-like) with two order parameters. One is related to the particle density while the second is the usual nematic order parameter in its scalar form (uniaxial mesophase). Specific anisotropic interactions between the particles are not taken into account. We attempt to classify the different phase diagrams arising on varying the coupling strength, which is related to the particle size under strong anchoring. Finally, section 4 is devoted to a short discussion and concluding remarks and wide perspectives envisaged after this preliminary study.

We now present our experimental results.

2. Experimental results.

As mesophase matrix we have chosen an aqueous lyotropic system in order to favour the dispersion of latex polyballs which are usually hydrophylic. A second advantage of the lyotropic system is that the elastic constants are weaker than those of thermotropic systems, reducing then the energetic cost to pay for the distortion of the nematic director field generated by the particles. Moreover, these elastic constants may be varied over some range by adjusting the surfactant concentration, giving some freedom to control the elastic interactions if necessary.

Among the different lyotropic liquid crystals extensively studied, the binary mixture of cesium pentadecafluorooctanoate (CsPFO) and water is certainly the simplest [25]. No cosurfactants or salt are necessary to stabilize non-spherical micelles. This system is of special interest because it exhibits a micellar nematic phase N_D of discoid type over a large range of concentration and temperature, ranging from about 0.2 to 0.65 weight fraction in surfactant and from 12 to about 70 °C [25]. This phase is intermediate to a lamellar phase L_α at lower temperatures and an isotropic micellar phase L_1 at higher temperatures. Note that the L_1-N_D transition is weakly first order while the N_D-L_a transition is second order over most of the N_D composition range. Typically the aspect ratio a/b of discoid micelles is in the range of 0.2-0.55, depending on the temperature and surfactant concentration with $a = 2.2$ m.

CsPFO was prepared by neutralizing an aqueous solution of pentadecafluorooctanoic acid (Aldrish Ltd.) with ceasium carbonate (Aldrish Ltd.). The neutralized solution was evaporated to dryness and the salt was recrystallized from ethanol. The samples were prepared by weighing CsPFO and aqueous suspensions of latex polyballs. Two types of dispersion of different particle size were used, both being a generous gift from Dr. Joanicot (Rhône-Poulenc company). The diameters of monodisperse latex particles from each batch were 120 and 60 nm. The polymer used for the latex is a styrene-butyl acrylate-acrylate acid copolymer. The latex spheres were charged by carboxylic acid groups grafted onto the surfaces, with a charge density of 260 μEq/g.

We do not expect significant changes in the CsPFO concentration due to adsorption onto the latex particles at the concentrations used for the samples studied. Even in the highly unlikely

case (latex particles and surfactant are both negatively charged in water) of a full covering of polyballs with the surfactant, for a typical concentration of 3 wt% and 40 wt% respectively in particles and CsPFO, the order of the surfactant loss is 0.001 of its total amount in solution.

2.1 DOPING WITH LARGE PARTICLES. — We now describe the phase diagram obtained with the two types of latex particles. We consider only cuts of the ternary diagram, keeping the ratio of the amount of surfactant over water constant and varying the latex volume fraction and the temperature. First, let us describe the phase diagram obtained with the larger polyballs. Although only one cross-section at fixed molecular ratio of surfactant to water has been extensively investigated, many complementary observations at different molecular ratios suggest that the phase behavior with these large lattices is similar over most of the range of the nematic phase. The stability of the suspension was characterized both by optical microscopy and by macroscopic observation of bulk properties of a few grammes of the sample as a function of temperature. After any change in temperature, sample turbidity and birefringence were noted over the course of hours to determine precisely the phase separations and transitions.

As long as the solvent is in the isotropic state, the latex particles are well-dispersed, giving weakly turbid solutions in the case of dilute samples and quite opaque and white solutions as the doping volume fraction, ϕ_l, is increased. This first result indicates that, firstly the electrostatic repulsion between the latex spheres is still efficient in spite of the screening arising from the dissociated surfactants [26], and secondly the depletion of micelles yields only a weak attraction as expected when the ratio of the diameters of the two solutes is just ten or so [27].

Whatever the latex content of the solution, as soon as the isotropic-nematic transition temperature is reached from above, a liquid-liquid phase separation occurs (or a liquid-solid phase separation for higher ϕ_l and for deep quenches). In a vial, a clear, translucent and birefringent volume settles to the bottom while a very white and opaque volume creams up to the top. This second result indicates that the latex content of the nematic phase is rather low, i.e. the latex segregation into isotropic phase is fairly complete. The volume fraction of the cream decreases as the temperature decreases. Observation under a microscope of samples sandwiched between two sealed slides confirms the preceding conclusion. When the transition temperature is reached, a uniform nucleation of nematic droplets occurs across the sample. While the nematic droplets grow their interfaces push away the lattices through more and more concentrated regions. During the coarsening of the nematic droplets, domains concentrated in latex balls are finally isolated, making islands of various shapes with smooth edges. But the morphology of these flocs relaxes to a spherical shape after a few minutes, indicating that the latex particles contained inside are in a liquid state. No macroscopic fluctuations of shapes have been observed, even very close to the transition. As the droplet sizes are often larger than a few microns and the viscosity of lyotropic nematic phase is typically a few poises [28, 29], the droplets do not display noticeable Brownian motions. During the phase separation process, coalescence of flocs can occur especially in the early stages, giving rise to larger droplets which reach the steady spherical shape after a while. To summarize, at a given temperature below the transition temperature, the sample appears under a microscope as a dispersion of polydisperse, macroscopic, isolated and motionless droplets surrounded by a nematic medium, almost free of isolated latex particles, as illustrated by the photomicrograph shown in figure 1a.

When the temperature is further decreased into the nematic domain, small birefringent droplets are expelled from the fluid flocs. These nematic droplets can coalesce amongst themselves inside the flocs, before coalescing with the nematic matrix. The volume of the latex flocs is then reduced while their optical contrast with the surrounding medium is enhanced.

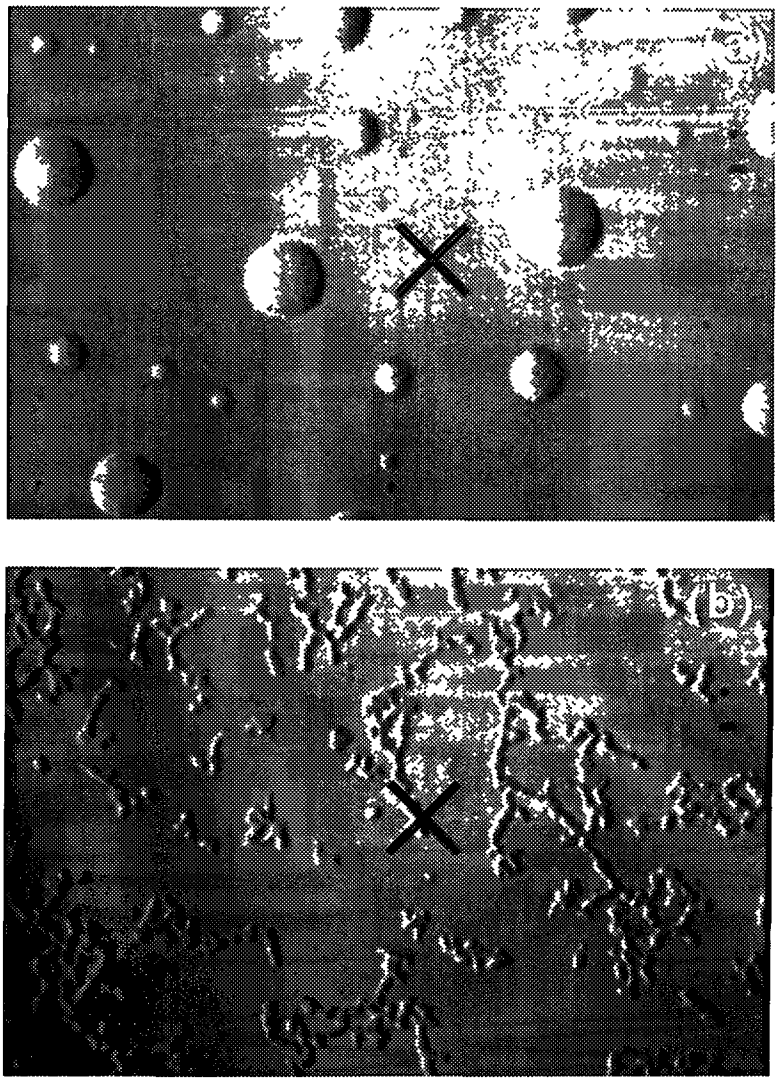

Fig. 1. — Below the isotropic-nematic transition, the 120 nm latex particles cluster a) near the transition in spherical fluid flocs and b) far from the transition in fractal solid aggregates. The surrounding nematic medium is free of isolated latex particles.

This behavior is completely reversible. On going back to higher temperatures the flocs swell back to their initial size. Below some well-defined temperature, the latex flocs lose their liquid nature. Gradually, the latex particles become motionless, this process starts at the core of the flocs and then spreads to the edges. When the flocs are solid-like, they become slightly more irregular, their edges seem to facet, and the collision of two of them results now in sticking and no longer in coalescence. There is no noticeable change in their size on further decrease in the temperature. A deep quench from a one-phase temperature to these temperatures where the flocs are rigid, generates aggregates very different in shape. The aggregation is then controlled by the coarsening process of the nematic phase, giving rise to very irregular fractal-like aggregates, as shown in figure 1b. When the concentration in latex particles is large enough,

the aggregates tend to connect in an infinite network. Under heating, the multi-branched aggregates melt back into the fluid droplets. This process starts from the edges. The aggregate arms melt first and give droplets with a fluid outer shell. Their solid cores melt some time later.

A usual technique to determine the (T, ϕ_l) cut plane of the phase diagram would be to measure the respective volume of each phase *versus* the temperature in a vial containing a few grammes of the sample. With the present system, owing to its high viscosity, reaching equilibrium is tedious. Indeed, after demixion, the denser nematic phase which is free of latex particles needs always many days to sediment to the bottom. Note also that this technique is doubtful when the solid flocs make some rigid networks as observed a few degrees below the isotropic-nematic transition. A much faster alternative technique, owing to the much smaller volumes involved, is to follow under a microscope the size of the spherical flocs in which the latex particles are trapped. In a three-dimensional space, with uniform spherical latex particles, the dependence of the volume fraction of particles ϕ_l on the floc radius R, is given by

$$\phi_l = \phi_c (R_c/R)^3 \tag{1}$$

where ϕ_c is the characteristic closest packing fraction of an array (i.e. 0.7405 for hexagonal, 0.5236 for simple cubic, etc..) while R_c is the ultimate radius of a floc at the close packing density. Consequently, successive measurements under cooling of the radii of a few flocs, down to the temperatures at which the solid floc radii become fixed and equal to R_c, give the ratio of the volume fraction of insertions to the constant close packing density. Since, according to the microscopic observation, the solid content of the nematic phase is always zero, a phase diagram in the $(t, \phi_l/\phi_c)$ plane is obtained where t is the temperature shift from the isotropic-nematic transition, $T - T_c$. A typical phase diagram is given in figure 2, for the following sample composition, 26 wt% CsPFO, 73.25 wt% H_2O and 0.75 wt% latex particles. The isotropic-nematic transition temperature T_c has been measured to be 19.68 °C. Around 18.75 °C, 1 °C below the demixion temperature (Fig. 2), the flocs become solid-like and get their minimal size. Just below the transition temperature, i.e. at $t = -0.02$ °C, the closest approach allowed by our experimental set-up, the size of the fluid droplets were found to be about 2.8 times larger than that at 1 °C below the transition (Fig. 3).

Let us now consider the case of smaller doping particles.

2.2 DOPING WITH SMALL PARTICLES. — In this section we report the results obtained with the 600 Å particles. These polyballs can be suspended both in the isotropic and nematic phases, giving the so-called IL and NL one-phases. Each homogeneous one phase will be named by a two letter abbreviation ; the first one stands for the state of the solvent (N or I for nematic or isotropic medium) while the second letter stands for the state of the particle dispersion (L or S for liquid or solid). The 600 Å particle phase diagram being much more complex than the preceding one, we will restrict our consideration to the general trends, keeping the extensive description [30] for a forthcoming paper. Let us start with an example to definitively prove the existence of the NL phase.

Towards this goal, we consider the particular sample whose composition is 39.4 wt% CsPFO, 59.9 wt% H_2O and 0.7 wt% latex particles. The isotropic-nematic transition temperature was found to be 34.5 °C, the transition being slightly more strongly first order than in the sample free of particles. Indeed, the range of the biphasic domain is expanded from about 0.1 °C without lattices to 0.6 °C with them. Contrary to the preceding system, the two coexisting phases are turbid, suggesting that latex particles are suspended both in the nematic and in the isotropic phases. The NL one phase extends from 33.9 °C down to 31.6 °C. No macroscopic phase separation is observed over the course of weeks at these temperatures. Below 31.6 °C, a network texture emerges (see below) under microscope, but above, in the

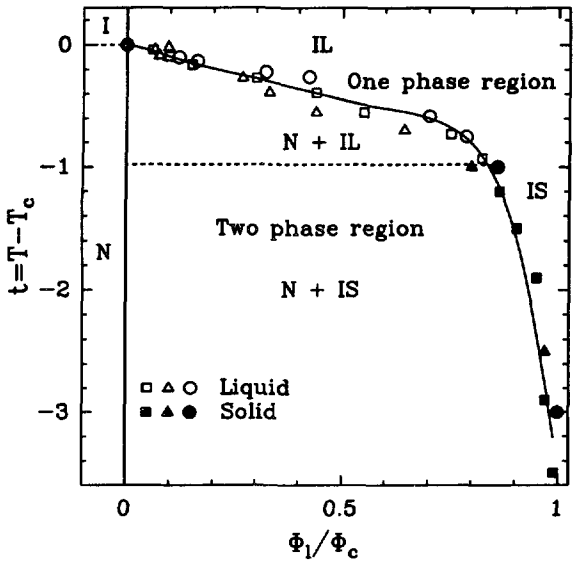

Fig. 2. — Temperature *versus* latex concentration phase diagram cut obtained with three different spherical flocs of 120 nm latex particles (see text). The floc solid state was detected by the cessation of the motion of latex particles in the droplets. T_c the isotropic-nematic transition temperature with the initial 0.75 w% latex particles was 19.7 °C. ϕ_c is the closest packing fraction of lattices in the solid flocs at low temperatures. The two-phase region corresponds to an equilibrium between a nematic phase free of latex particles and an isotropic phase containing all the latex particles. Above the solid line the phase is homogeneous and isotropic.

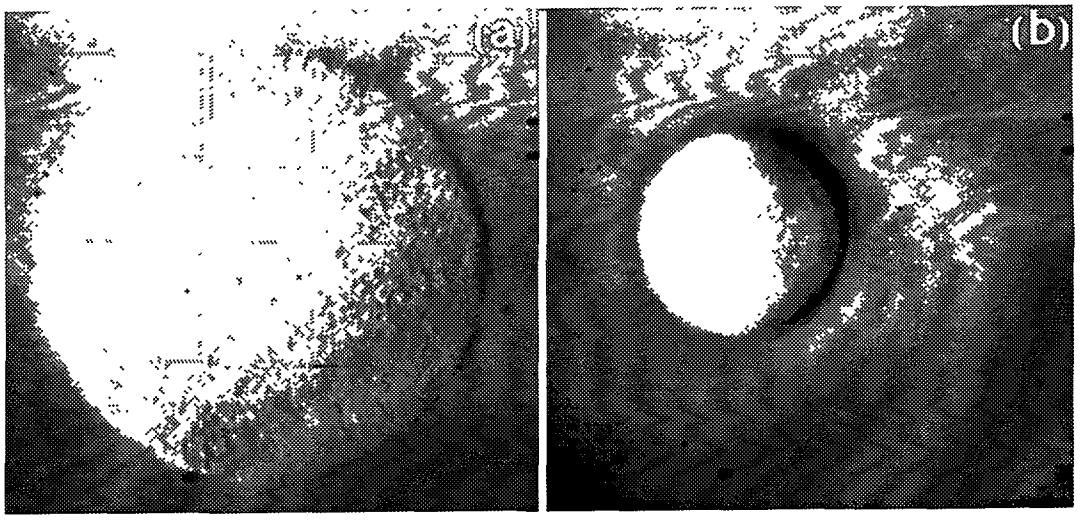

Fig. 3. — Same spherical floc containing several hundreds of 120 nm latex particles a) swollen near the isotropic-nematic transition and b) shrunk one degree lower.

one phase temperature range, absolutely no latex flocs are observed. However an ordinary optical microscope does not allow to distinguish such small particles and likewise aggregates of a few particles to be distinguished. In order to definitively check whether the doping particles remain well dispersed in the NL phase, we measured the Brownian diffusion coefficient of particles by dynamic light scattering. As illustrated in figure 4, both in the isotropic and the nematic solvent, the characteristic relaxation frequencies of the density fluctuations were found to be proportional to the square of the scattering vector. The temperatures of measurement were shifted by almost three degrees on either side of the isotropic-nematic transition. The diffusion coefficient in the isotropic phase is about 1.4 times that in the nematic phase, which is consistent with an increase of the global viscosity as checked with a rheometer, namely about 54 cp for the IL phase and 73 cp for the NL phase. From the latter results, and from the macroscopic and the microscopic observations we can definitively conclude that the 600 Å lattices are in suspension in the nematic matrix.

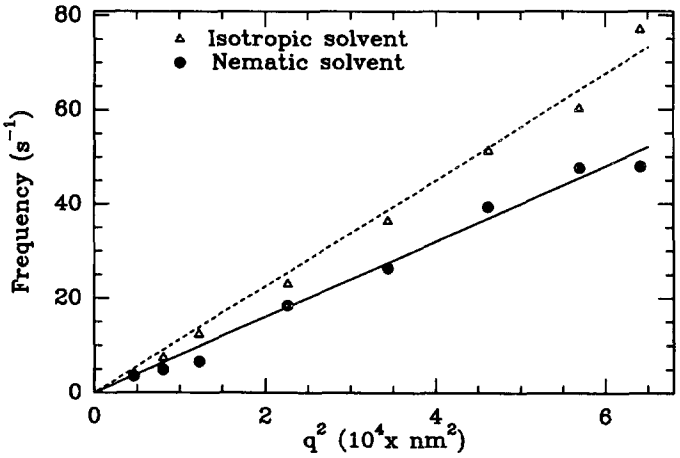

Fig. 4. — Dynamic light scattering measurements of the relaxation frequencies of the 60 nm latex particles suspended in the isotropic and in the nematic solvent. The diffusion coefficients were found to be 11.5×10^4 nm^2 s^{-1} and 8.1×10^4 nm^2 s^{-1} respectively in the two phases.

The maximum of latex particles allowed in the nematic phase depends on the molecular ratio of the surfactant to water. The larger the surfactant fraction, the larger the volume fraction of particles. In the most favorable case, up to more than 7 wt% latex particles have been kept dispersed. Under cooling, before reaching the lamellar phase, the doping particles interact strongly amongst themselves, giving what is perceived under the microscope as a steady greyish texture, similar to a frozen spinodal decomposition pattern in its first stage. A photomicrograph of such a pattern is shown in figure 5. The characteristic mesh size of the texture grows as the temperature is decreased. However, under heating, this behavior is fully reversible, attesting to the thermodynamic nature of these patterns. The higher the solid content, the closer from the isotropic-nematic transition the occurrence of these patterns. Finally, what is more intriguing is that the nematic matrix can always be well oriented between slides, in spite of the dispersed particles and the texture at low temperatures, even in the concentrated regime (up to about 3 %w particles).

We now wish to account for the behavior of the two systems by developing a simple model.

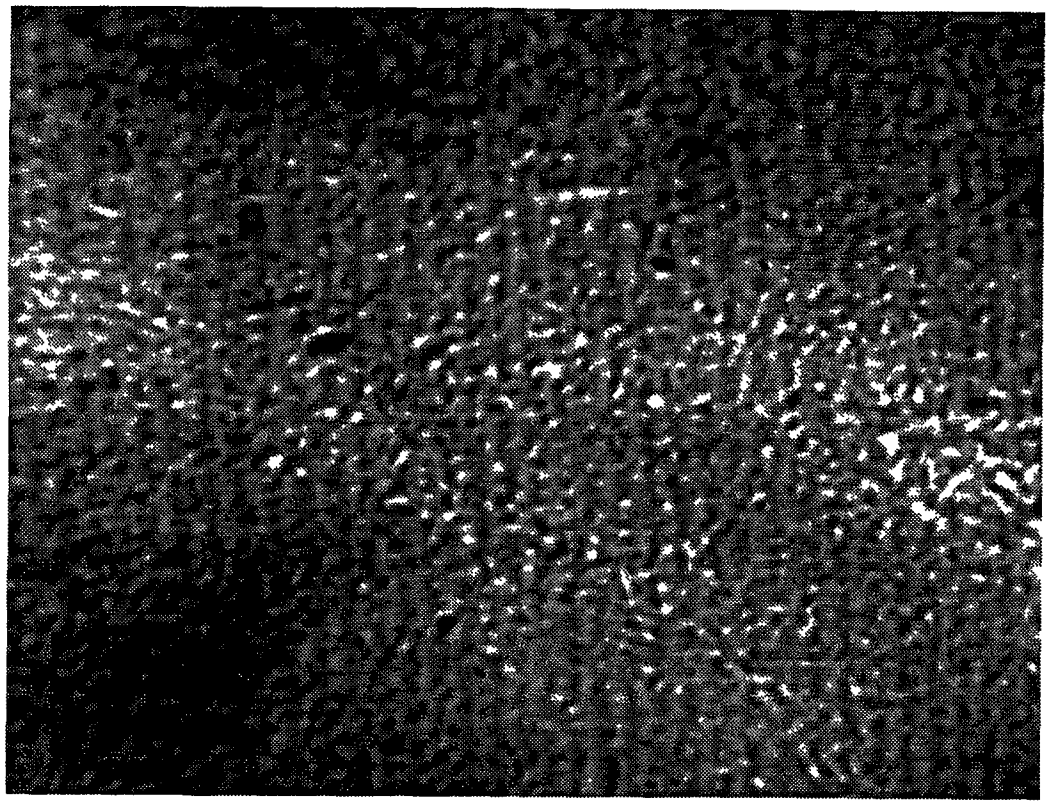

Fig. 5. — Characteristic texture emerging a few degrees below the isotropic-nematic transition, suggesting that the 60 nm latex particles suspended in the nematic solvent interact with specific forces to aggregate at some precise temperature.

3. Landau expansion and phase diagrams.

The system we consider here is made of a suspension of monodisperse hard sphere particles dispersed in a nematic matrix. We will examine it in the vicinity of the nematic-isotropic transition. The nematic solvent is chosen uniaxial so that the related second rank tensor order parameter can be reduced to a scalar in a suitable coordinate system.

Our starting point is the following Landau expansion of the Helmholtz free energy density :

$$f(Q, \phi) = \frac{1}{2} a(T) Q^2 - \frac{c}{3} Q^3 + \frac{d}{4} Q^4 + \frac{k_B T}{V} (\phi \ln \phi + \phi^2(4 - 3\phi)/(1 - \phi^2)) + \frac{k}{2} Q^2 \phi \, . \tag{2}$$

Three distinct contributions can be distinguished : the energy density of the solvent alone f_N, the energy density of the particle suspension f_P, and a coupling term f_C which links the two. Let us discuss each one

$$f_N(Q) = \frac{1}{2} a'(T - T_0) Q^2 - \frac{c}{3} Q^3 + \frac{d}{4} Q^4 \tag{3}$$

is the usual Landau expansion in the mean field approximation which describes the first order isotropic-nematic transition [31]. The coefficients a', c and d are positive. The order parameter Q is defined as $Q = \frac{1}{2} \langle 3 \cos^2 \theta - 1 \rangle$ where θ is the angle between the director $\mathbf{n}$ and the molecular axis vector $\mathbf{u}$ [31]. The average is over a small macroscopic volume. The equilibrium value of Q is zero in the isotropic phase and is between zero and one in the nematic phase

$$f_P(\phi) = \frac{k_B T}{V} (\phi \ln \phi + \phi^2(4 - 3\phi)/(1 - \phi^2)) \tag{4a}$$

is the Carnaham-Starling free energy density of a fluid suspension of spheres interacting together by steric repulsion [32], ϕ being the volume fraction of particles. At high sphere concentration, $\phi > \phi^*$, when the particles are in solid state, f_P can be rewritten as [33]

$$f_P(\phi) = \frac{k_B T}{V} (u_0 \phi + 3 \phi \ln (\phi/(1 - \phi/\phi_c))) \tag{4b}$$

where u_0 is an adjustable parameter so that (4a) = (4b) at $\phi^* (\approx 0.52)$, and ϕ_c is the closest packing fraction.

An important choice in defining our Landau expansion concerns the coupling term,

$$f_C(Q, \phi) = \frac{k}{2} Q^2 \phi . \tag{5}$$

Here we have retained only the lowest order term of the coupling. From a purely formal standpoint, since Q has a tensorial origin, the lowest power in Q to be homogeneous in rank is necessarily two since ϕ is itself a scalar. On the other hand, from a physical standpoint, $kQ^2/2$ can be seen at zero order as the distortion cost that every doping particle produces in the nematic director field. A precise relation for the coupling coefficient is not straightforward to establish. Among the relevant parameters we can mention the elastic constants of the nematic solvent, the diameter of the particles and also the direct interactions between the nematic molecules and the inclusions, i.e. the anchoring conditions. Under strong anchoring, the coupling coefficient is expected to be directly proportional to the particle radius, $kQ^2 \propto KR/V$, where K is a linear combination of the three nematic elastic moduli depending on the nature of the alignment [31]. Notice from (2) that since $k > 0$, as expected for spherical doping particles, the isotropic-nematic transition would be delayed as the doping concentration is increased. The elastic cost per unit is proportional to ϕ as long as no specific interactions between the distorted layers around each particle are considered. $kQ^2/2$ can be seen as the excess chemical potential of the particles in the nematic phase. Coupling terms of higher order in ϕ should be included in (5) to take into account the interactions mediated by the nematic solvent. In this preliminary study we neglect these specific interactions though experimentally it seems we have some evidence for them.

It is helpful to derive the possible topologies of phase diagrams directly from (2) by using the common tangent rule in (T, ϕ) space, corresponding to the suitable experimental parameters. Phase diagrams are calculated by the following method ; $f(Q, \phi)$ is first minimized with respect to variations in Q, thus defining a function of one variable $f(\phi) = f(\phi, \bar{Q}(\phi))$ where $\bar{Q}(\phi)$ is the value of Q for which f is minimized at a given ϕ. The common tangent construction may now be applied to the minimized function $\bar{f}(\phi)$. Analytically, if there is a multiphase coexistence, the common construction corresponds to satisfying both the chemical potential $\mu_i = (\partial f/\partial \phi)_i$ and the osmotic pressure $P_i = f(\phi_i) - \phi_i \mu_i$ conditions,

$u_i = u_j = \cdot$ and $P_i = P_j = \cdot$ where ϕ_i refer to the respective volume fractions of particles in each phase.

On minimizing $\bar{f}(Q, \phi)$ with respect to Q, we simply obtain,

$$\begin{aligned} \bar{Q}(\phi) &= 0 && \phi \geqslant \phi_{Tr} \\ \bar{Q}(\phi) &= \frac{c + \sqrt{c^2 - 4\,d(a + k\phi)}}{2\,D} && \phi < \phi_{Tr} \end{aligned} \tag{6}$$

with $\phi_{Tr} = 2\,c^2/(9\,dk) - a/k$. Note that if $T > T_0 + 2\,c^2/(9\,da')$ then $\bar{Q}$ is always equal to zero whatever the particle volume fraction ϕ. Although the calculations on the minimized free energy $\bar{f}(\phi)$ are mainly analytical, at some points a straightforward numerical treatment is required. Actually a good qualitative feeling for the phase diagrams can be obtained just by plotting the function $\bar{f}(\phi)$ at fixed value of T and looking for common tangents.

Let us now describe the phase diagrams obtained at different coupling strengths, keeping fixed the other parameters, a', T_0, c and d. Three phase diagrams in the plane (T, ϕ) are displayed in figure 6 corresponding to weak, moderate and strong coupling. In varying the coupling coefficient k we can pass smoothly from one to another. Four thermodynamic one-phases emerge in the phase diagrams. The IL and NL phases are homogeneous dispersions of latex, respectively in an isotropic and nematic medium. Above a concentration threshold in particles, the latex organization is solid-like, leading to the IS and NS phases following the nature of the surrounding solvent.

A common characteristic of the phase diagrams is that the transition temperature is lowered as the colloidal particle concentration is increased as one would expect intuitively. Each particle generates some degree of disorder around itself (the coupling coefficient is positive), depending on the coupling strength, delaying locally the nematic structuration. The second remark is that the isotropic-nematic transition becomes more first order when particles are added, especially under strong coupling. For weak coupling, the first order character is just slightly enhanced at the smaller doping concentrations (Fig. 6a). On the other hand, for strong coupling, the transition becomes so much strongly first order (Fig. 6c), that almost all the particles can be excluded from the nematic phase and kept inside the isotropic one.

For weak and moderate coupling, the diagrams exhibit two triple points, for $a = a_1$ and a_2 (Fig. 6). The former a_1 corresponds to the coexistence between the phases IL, NL and IS,

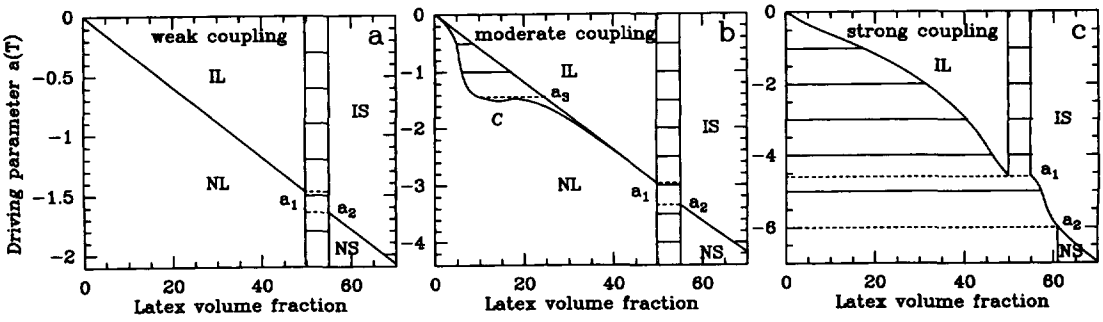

Fig. 6. — Theoretical phase diagrams obtained with (2) at different coupling strengths with the following numerical values ; $kT/V = 1.0$, $c = 0.3$, $d = 1.0$, and $a' = 1.0$. The one phase domains are named by a two letter abbreviation (see text) while the two phase regions are shaded. a) weak coupling : $k = 3.0$, b) moderate coupling : $k = 6.0$, and c) strong coupling : $k = 10.0$.

while the latter a_2 corresponds to the coexistence between the phases NL, NS and IS. Under strong coupling, the NL and the NS one phases disappear in favour of a pure nematic one phase since the particles are all expelled from the nematic matrix. Then the preceding triple points correspond to the coexistence with a N phase instead of NL phase. A remarkable feature for moderate coupling is the emergence of new equilibria between two phases of type NL providing the critical point C (Fig. 6b). Since no extra specific attractive interactions have been considered in the free energy (2), the coupling under consideration is enough to drive the second virial coefficient negative. However, a relevant test of this conclusion requires adding ϕ^2 interaction terms in order to be consistent in the expansion (2). When $a = a_3$ the new triple point corresponds to the equilibrium between the two NL phases together with the IL phase.

4. Conclusion.

The model allows us to gain some insights into the preceding experimental observations. Both the sign and the magnitude of the coupling term in (2) are crucial in the behavior at the isotropic-nematic transition. As we have already mentioned, k is suspected to be positive for spherical inclusions, because spherical particles would induce disorder in the nematic director field. In consequence this term does not favor the transition to the nematic phase but rather delays it, the drop in the transition temperature being greater for stronger coupling and larger latex volume fraction. This feature has been observed with both large and small particles and is illustrated in figure 2. The strength of the coupling term determines the width of the two phase region. The stronger the coupling term, the larger the coexisting phase domain as illustrated in figure 6. As we have already mentioned, the coupling term can be regarded as an exchange chemical potential, characterizing the cost in free energy of transferring a spherical particle from the isotropic to the nematic solvent. In consequence the system has some advantage in concentrating the latex in the isotropic phase, in spite of the loss in mixing entropy, thereby making the chemical potential in the two coexisting phases equal. But concentrating too much can become too penalizing in terms of particle interaction so that the particles are definitively admitted in the nematic phase. The stronger the coupling term, the higher the concentration at which the dispersion in the nematic phase occurs. For too strong couplings the balance is never reached and the particles aggregate outside the nematic phase, giving a complete segregation like that we have observed with the larger particles.

In conclusion, we have experimentally verified that the dispersion of solid spherical particles in a nematic matrix is workable, provided that the particle size is not too large whereby the energy of the distorted volume stays limited. A simple two order parameter Landau expansion accounts for such a behavior. The interaction between the two order parameters controls the particle segregation at the isotropic-nematic transition. This model must be extended, notably by adding some specific interaction terms with respect to the anisotropic nature of the solvent. Thereby we can expect to account for the structuration responsible for the texture observed in the nematic phase. Unfortunately to express analytically even with some approximations the elastic interactions between two spheres immersed in a 3D nematic medium is not a straightforward task, with both planar and homeotropic alignments. However numerical simulations may bring some insights in order to model these anisotropic interactions. Some attempts are currently underway in this direction.

However we did not yet explicitly show that the force responsible for the structuration was a specific interaction mediated by the anisotropic solvent. Taking advantage of the fact that these doped systems align quite easily in thin slabs, scattering techniques, especially using neutrons, would allow us to test the anisotropy of the macroparticle doublet interactions. Another exciting experimental extension would be the study of the consequences of the inclusions on

the physical properties of the nematic matrix. Special attention should be paid to the viscoelastic characteristic of the system.

Acknowledgements.

It is a pleasure to acknowledge stimulating discussions with Claude Coulon, Frédéric Nallet, Jacques Prost, and Sriram Ramaswamy. This work was funded in part by an Indo-French cooperation grant (IFCPAR through Grant No 607-1). We thank Rhône-Poulenc company and Dr. Joanicot for providing us with the latex particles and Françoise Argoul for her help in digitizing the pictures.

References

[1] Zocher H., *Z. Anorg. Allg. Chem.* **147** (1925) 91.
[2] Bondy C., *Trans. Far. Soc.* **35** (1939) 1093.
[3] Luck W., Klier M. and Wesslaw H., *Naturwiss* **50** (1963) 485.
[4] Hachisu S., Kobayashi Y. and Kose A., *J. Colloid Interface Sci.* **42** (1973) 342.
[5] Hachisu S. and Kobayashi Y., *J. Colloid Interface Sci.* **46** (1974) 470.
[6] Long J. A., Osmond S. W. J. and Vincent B., *J. Colloid Interface Sci.* **42** (1973) 545.
[7] Asakura S. and Oosawa F., *J. Chem. Phys.* **22** (1954) 1255.
[8] Vincent B., Luckham P. F. and Waite F. A., *J. Colloid Interface Sci.* **73** (1980) 508.
[9] de Hek H. and Vrij A., *J. Colloid Interface Sci.* **84** (1981) 409.
[10] Zimmermann U., *Biochem. Biophys.* **694** (1982) 227.
[11] Skjeltorp A. T., *Phys Rev. Lett.* **51** (1983) 2305.
[12] Richetti P., Prost J. and Clark N. A., Physics of Complex and Supermolecular fluids, S. A. Safran and N. A. Clark Eds. (Wiley-Interscience, 1987) p. 387.
[13] Horn R. G., Israelachvili J. N. and Perez E., *J. Phys. France* **42** (1981) 39.
[14] Richetti P., Kékicheff P., Parker J. L. and Ninham B. W., *Nature* **346** (1990) 39.
[15] Marčelja S. and Radic N., *Chem. Phys. Lett.* **42** (1976) 129.
[16] Poniewierski A. and Sluckin T. J., *Liq. Cryst.* **2** (1987) 281.
[17] de Gennes P. G., *Langmuir* **6** (1990) 1448.
[18] Ajdari A., Peliti L. and Prost J., *Phys. Rev. Lett.* **66** (1991) 1481 ;
Ajdari A., Duplantier B., Hone D., Peliti L. and Prost J., *J. Phys. II France* **2** (1992) 484.
[19] Kosterlitz J. M. and Thouless D. J., *J. Phys C* **6** (1973) 1181.
[20] Lammert P. E., Rohshar D. S. and Toner J., *Phys. Rev. Lett.* **70** (1993) 1650.
[21] Kreuzer M., Tschudi T. and Eidenschink R., *Mol. Cryst. Liq Cryst.* **223** (1992) 219.
[22] Brochard F. and de Gennes P. G., *J. Phys. France* **31** (1970) 691.
[23] Chen S. and Amer N. M., *Phys. Rev. Lett.* **51** (1983) 2298.
[24] Figueiredo Neto A. M. and Saba M. M. F., *Phys. Rev. A* **34** (1986) 3483.
[25] Boden N., Jackson P. H., McMullen K. and Holmes M. C., *Chem Phys. Lett.* **65** (1979) 476.
[26] Richetti P. and Kékicheff P., *Phys. Rev. Lett.* **68** (1992) 1951.
[27] Bibette J., Roux D. and Nallet F., *Phys. Rev. Lett.* **65** (1990) 2470 ;
Bibette J., Roux D. and Pouligny B., *J Phys. France II* **2** (1992) 401.
[28] Haven T., Armitage D. and Saupe A., *J. Chem. Phys.* **75** (1981) 352.
[29] Kumar S., Yu L. J. and Lister J. D., *Phys. Rev. Lett.* **50** (83) 1672.
[30] Raghunathan V. A., Richetti P. and Roux D., in preparation.
[31] de Gennes P. G., Physics of liquid crystals (Oxford University, London, 1974).
[32] Carnaham N. F. and Starling K. E., *J. Chem. Phys.* **51** (1969) 635.
[33] Russel W. B., Saville D. A. and Schowalter W. R., Colloidal Dispersions (Cambridge University, Cambridge, 1989).